Parameter identification for active mass damper controlled systems

Parameter identification for active mass damper controlled systems

C C Chang[1] , J F Wang[2], and C C Lin[3]

[1] Assistant Researcher, National Center for Research on Earthquake Engineering, National Applied Research Laboratories, 200, Sec. 3, Xinhai Rd., Taipei 10668, Taiwan, R.O.C. ccchang@ncree.narl.org.tw

[2] Assistant Research Fellow, 921 Earthquake Museum of Taiwan, National Museum of Natural Science, Taichung 41364, Taiwan, R.O.C.

[3] Distinguished Professor, Department of Civil Engineering, National Chung Hsing University, Taichung 40227, Taiwan, R.O.C.

Abstract. Active control systems have already been installed in real structures and are able to decrease the wind- and earthquake-induced responses, while the active mass damper (AMD) is one of the most popular types of such systems. In practice, an AMD is generally assembled in-situ along with the construction of a building. In such a case, the AMD and the building is coupled as an entire system. After the construction is completed, the dynamic properties of the AMD subsystem and the primary building itself are unknown and cannot be identified individually to verify their design demands. For this purpose, a methodology is developed to obtain the feedback gain of the AMD controller and the dynamic properties of the primary building based on the complex eigen-parameters of the coupled building-AMD system. By means of the theoretical derivation in state-space, the non-classical damping feature of the system is characterized. This methodology can be combined with any state-space based system identification technique as a procedure to achieve the goal on the basis of the acceleration measurements of the building-AMD system. Results from numerical verifications show that the procedure is capable of extracting parameters and is applicable for AMD implementation practices.

1. Introduction

In recent years, remarkable progress has been made in the field of active control of civil engineering structures subjected to environmental loadings such as winds and earthquakes [1, 2]. Various control methods were proposed with new control devices to different civil engineering structures. Among them, the active control method has attracted intensive theoretical and experimental attention[3-7]. Since the application of active control in civil engineering field in 1970 [8], several control approaches have been investigated, such as LQ [7,9], LQR [6,10], and H_∞ control [11-13]. Active control systems have already been installed in real structures and are able to decrease the wind- and earthquake-induced responses, while the active mass damper (AMD) is one of the most popular types of such systems. In practical, an AMD is generally assembled in-situ along with the construction of a building.

However, there are still many issues to be solved for active control techniques towards real implementation, such as system instability due to inappropriate selection of control parameters and control force execution time delay, which may significantly deteriorate the control performance. In such a case, the AMD and the building is coupled as an entire system. After the construction is completed, the dynamic properties of the AMD subsystem and the primary building itself are unknown and cannot be identified individually to verify their design demands. For this purpose, a methodology is developed to obtain the feedback gain of the AMD controller and the dynamic properties of the primary building based on the complex eigen-parameters of the coupled building-AMD system. By means of the theoretical derivation in state-space, the non-classical damping feature of the system is characterized. This methodology can be combined with any state-space based system identification technique as a procedure to achieve the goal on the basis of the acceleration measurements of the building-AMD system. Results from numerical verifications show that the procedure is capable of extracting parameters and is applicable for AMD implementation practices.

2. AMD-controlled systems

2.1. Equations of motion of AMD-controlled system

For a n-DOF discrete-parameter structure with a AMD attached on the lth DOF subject to dynamic loadings and active control forces, as shown in figure 1. The equations of motion take the form as

$$\mathbf{M}\ddot{\mathbf{x}}(t)+\mathbf{C}\dot{\mathbf{x}}(t)+\mathbf{K}\mathbf{x}(t)=\mathbf{E}_1\mathbf{w}(t)+\mathbf{B}_1\mathbf{u}(t) \tag{1}$$

where $\mathbf{M}$, $\mathbf{C}$ and $\mathbf{K}$ are the $N\times N$ (where $N=n+1$) system mass, damping and stiffness matrices, respectively, and can be expressed in detail as

$$\mathbf{M}=\begin{bmatrix} m_{p_1} & & & & & & \\ & m_{p_2} & & & & & \\ & & \ddots & & & & \\ & & & m_{pl} & & & \\ & & & & \ddots & & \\ & & & & & m_{p_n} & \\ 0 & \cdots & m_s & \cdots & 0 & m_s \end{bmatrix}_{N\times N},\quad \mathbf{C}=\begin{bmatrix} c_{p_1}+c_{p_2} & -c_{p_2} & 0 & \cdots & \cdots & \cdots & 0 \\ -c_{p_2} & c_{p_2}+c_{p_3} & -c_{p3} & 0 & & & \vdots \\ 0 & \ddots & \ddots & \ddots & & & \vdots \\ \vdots & 0 & -c_{pl} & c_{p_l}+c_{p_{l+1}}+c_s & -c_{p_{l+1}} & 0 & -c_s \\ \vdots & & \ddots & \ddots & \ddots & \vdots & \vdots \\ \vdots & & & 0 & -c_{p_n} & c_{p_n} & 0 \\ 0 & \cdots & \cdots & \cdots & \cdots & 0 & c_s \end{bmatrix}_{N\times N},$$

$$\mathbf{K}=\begin{bmatrix} k_{p_1}+k_{p_2} & -k_{p_2} & 0 & \cdots & \cdots & \cdots & 0 \\ -k_{p_2} & k_{p_2}+k_{p_3} & -k_{p3} & 0 & & & \vdots \\ 0 & \ddots & \ddots & \ddots & & & \vdots \\ \vdots & 0 & -k_{pl} & k_{p_l}+k_{p_{l+1}}+k_s & -k_{p_{l+1}} & 0 & -k_s \\ \vdots & & \ddots & \ddots & \ddots & \vdots & \vdots \\ \vdots & & & 0 & -k_{p_n} & k_{p_n} & 0 \\ 0 & \cdots & \cdots & \cdots & \cdots & 0 & k_s \end{bmatrix}_{N\times N} \tag{2}$$

where m_{p_i}, and m_s represent the masses of the ith DOF and AMD, respectively; c_{p_i}, and c_s represent the damping coefficients of the ith DOF and AMD, respectively; k_{p_i}, and k_s represent the stiffness coefficients of the ith DOF and AMD, respectively. In addition, $\mathbf{x}(t)$ is the N-dimensional displacement vector, and can be expressed in detail as

$$\mathbf{x}=\{x_{p_1}\quad x_{p_2}\quad \cdots\quad x_{p_l}\quad \cdots\quad x_{p_n}\quad x_s\}^T_{N\times 1} \tag{2d}$$

where x_{p_i}, and x_s represent the displacement of the ith DOF and AMD relative to the ground, respectively. The notation $\mathbf{w}(t)$ is the r-dimensional external excitation vector and $\mathbf{u}(t)$ is the q-dimensional control force vector. The $n \times q$ matrix $\mathbf{B}_1$ and $n \times r$ matrix $\mathbf{E}_1$ respectively define the locations of control forces and excitations. In the situation of ground acceleration, $\ddot{x}_g(t)$, the $\mathbf{B}_1$ and $\mathbf{E}_1$ can be expressed as

$$\mathbf{B}_1 = \{0 \quad 0 \quad \ldots \quad -1^{(l)} \quad \ldots \quad 0 \quad 1\}^T_{N\times 1} \tag{2e}$$

$$\mathbf{E}_1 = \{-m_{p_1} \quad -m_{p_2} \quad \ldots \quad -m_{p_l} \quad \ldots \quad -m_{p_n} \quad -m_s\}^T_{N\times 1} \tag{2f}$$

Represented in state-space form, equation (1) can be rewritten as

$$\dot{\mathbf{X}}(t) = \mathbf{A}\mathbf{X}(t) + \mathbf{E}\ddot{x}_g(t) + \mathbf{B}\mathbf{u}(t) \tag{3}$$

where

$$\mathbf{X} = \begin{Bmatrix} \dot{\mathbf{x}} \\ \ddot{\mathbf{x}} \end{Bmatrix}, \ \mathbf{A} = \begin{bmatrix} \mathbf{0} & \mathbf{I} \\ -\mathbf{M}^{-1}\mathbf{K} & -\mathbf{M}^{-1}\mathbf{C} \end{bmatrix}, \ \mathbf{B} = \begin{Bmatrix} \mathbf{0} \\ -\mathbf{M}^{-1}\mathbf{B}_1 \end{Bmatrix}, \ \mathbf{E} = \begin{Bmatrix} \mathbf{0} \\ -\mathbf{M}^{-1}\mathbf{E}_1 \end{Bmatrix} \tag{4}$$

are $2N \times 1$ state vector, $2N \times 2N$ system matrix, $2N \times 1$ controller location matrix and $2N \times 1$ external excitation location matrix, respectively. In this paper, active control forces are determined using the $\mathbf{H}_\infty$ direct output feedback control theory developed by Lin *et al.* [11, 12].

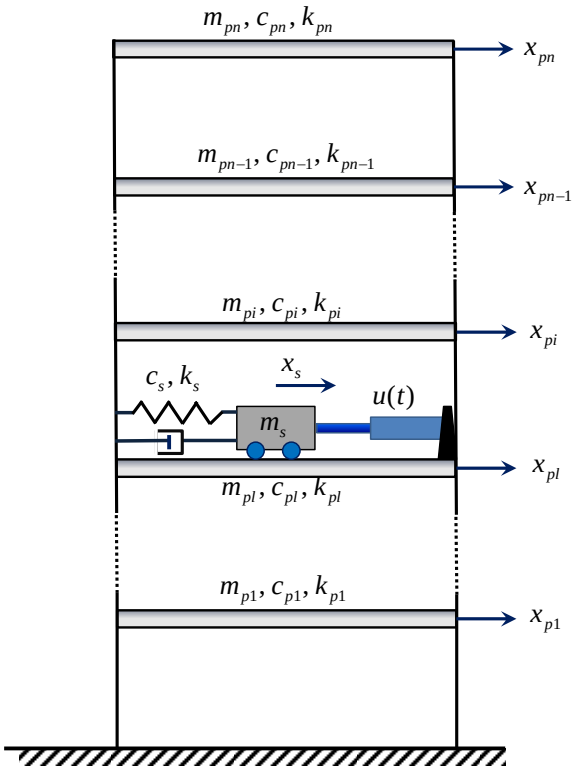

Figure 1. System model of a multistory building structure with AMD

2.2. $\mathbf{H}_\infty$ *direct output feedback control theory*

Define a $p\times 1$ control output vector $\mathbf{Z}(t)$ and an $s\times 1$ output measurement vector $\mathbf{y}(t)$ as

$$\mathbf{Z}(t)=\mathbf{C}_1\mathbf{X}(t)+\mathbf{D}\mathbf{u}(t) \tag{5}$$

$$\mathbf{y}(t)=\mathbf{C}_2\mathbf{X}(t) \tag{6}$$

where $\mathbf{C}_1$, $\mathbf{D}$ and $\mathbf{C}_2$ are $p\times 2N$, $p\times q$ and $s\times 2N$ matrices. The direct output feedback control force is calculated by

$$\mathbf{u}(t)=\mathbf{G}\mathbf{y}(t)=\mathbf{G}\mathbf{C}_2\mathbf{X}(t) \tag{7}$$

where $\mathbf{G}$ is a $q\times 2s$ time-invariant feedback gain matrix. According to H_∞ control algorithm, the H_∞ norm of transfer function matrix $\mathbf{T}_{\mathbf{Zw}}(j\omega)$ of control output $\mathbf{Z}(j\omega)$ with respect to external excitation $\mathbf{w}(j\omega)$ takes the form

$$\left\|\mathbf{T}_{\mathbf{Zw}}(j\omega)\right\|_\infty=\sup\frac{\left\|\mathbf{Z}(j\omega)\right\|_2}{\left\|\mathbf{w}(j\omega)\right\|_2} \tag{8}$$

where $j=\sqrt{-1}$, and sup is defined as the supremum over all $\mathbf{w}(t)$. According to the optimal H_∞ control algorithm (Yaesh and Shaked 1997), the H_∞ norm of transfer function matrix $\mathbf{T}_{\mathbf{Zw}}(j\omega)$ satisfies the following constraint

$$\left\|\mathbf{T}_{\mathbf{Zw}}(j\omega)\right\|_\infty=\sup\frac{\left\|\mathbf{Z}(j\omega)\right\|_2}{\left\|\mathbf{w}(j\omega)\right\|_2}<\gamma \tag{9}$$

where γ is a positive attenuation constant which denotes a measure of control performance. Adopting a smaller value of γ means that more stringent performance of control system is required. It has been proved [12] that an optimal H_∞ control system is asymptotically stable if there exists a matrix $\boldsymbol{P}\geq 0$ that satisfies the following Riccati equation

$$(\mathbf{A}+\mathbf{B}\mathbf{G}\mathbf{C}_2)^{\mathrm{T}}\mathbf{P}+\mathbf{P}(\mathbf{A}+\mathbf{B}\mathbf{G}\mathbf{C}_2)+\frac{1}{\gamma^2}\mathbf{P}\mathbf{E}\mathbf{E}^{\mathrm{T}}\mathbf{P}+(\mathbf{C}_1+\mathbf{D}\mathbf{G}\mathbf{C}_2)^{\mathrm{T}}(\mathbf{C}_1+\mathbf{D}\mathbf{G}\mathbf{C}_2)=\mathbf{0} \tag{10}$$

One way to design the optimal H_∞ output feedback gain is to solve Eq. (10) with minimizing the Entropy of $\mathbf{T}_{\mathbf{Zw}}(j\omega)$ which takes the form [11]

$$E_n(\mathbf{T}_{\mathbf{Zw}},\gamma)=tr\{\mathbf{E}\mathbf{E}^{\mathrm{T}}\mathbf{P}\mathbf{E}\} \tag{11}$$

where tr{-} denotes the trace of a square matrix. Then, the optimization problem to obtain gain matrix $\mathbf{G}$ is converted to minimize the Entropy in Eq. (11) subject to the constraint of Eq. (10). The Lagrangian L can be introduced as

$$L(\mathbf{G},\mathbf{P},\boldsymbol{\lambda})\equiv tr\left\{\mathbf{E}^{\mathrm{T}}\mathbf{P}\mathbf{E}+\boldsymbol{\lambda}[(\mathbf{A}+\mathbf{B}\mathbf{G}\mathbf{C}_2)^{T}\mathbf{P}+\mathbf{P}(\mathbf{A}+\mathbf{B}\mathbf{G}\mathbf{C}_2)+\frac{1}{\gamma^2}\mathbf{P}\mathbf{E}\mathbf{E}^{T}\mathbf{P}+(\mathbf{C}_1+\mathbf{D}\mathbf{G}\mathbf{C}_2)^{T}(\mathbf{C}_1+\mathbf{D}\mathbf{G}\mathbf{C}_2)]\right\} \tag{12}$$

where λ is a 8×8 Lagrangian multiplier matrix. For simplicity and without loss of generality, the necessary and sufficient conditions for minimization of $L(\mathbf{G},\mathbf{P},\boldsymbol{\lambda})$ are derived and expressed by

$$\frac{\partial L}{\partial\boldsymbol{\lambda}}=(\mathbf{A}+\mathbf{B}\mathbf{G}\mathbf{C}_2)^{\mathrm{T}}\mathbf{P}+\mathbf{P}(\mathbf{A}+\mathbf{B}\mathbf{G}\mathbf{C}_2)+\frac{1}{\gamma^2}\mathbf{P}\mathbf{E}\mathbf{E}^{\mathrm{T}}\mathbf{P}+(\mathbf{C}_1+\mathbf{D}\mathbf{G}\mathbf{C}_2)^{\mathrm{T}}(\mathbf{C}_1+\mathbf{D}\mathbf{G}\mathbf{C}_2)=0 \tag{13a}$$

$$\frac{\partial L}{\partial\mathbf{P}}=(\mathbf{A}+\mathbf{B}\mathbf{G}\mathbf{C}_2+\frac{1}{\gamma^2}\mathbf{E}\mathbf{E}^{\mathrm{T}}\mathbf{P})\boldsymbol{\lambda}+\boldsymbol{\lambda}(\mathbf{A}+\mathbf{B}\mathbf{G}\mathbf{C}_2+\frac{1}{\gamma^2}\mathbf{E}\mathbf{E}^{\mathrm{T}}\mathbf{P})^{\mathrm{T}}+\mathbf{E}\mathbf{E}^{\mathrm{T}}=0 \tag{13b}$$

$$\frac{\partial L}{\partial \mathbf{G}} = \mathbf{B}^{\mathrm{T}}\mathbf{P}\boldsymbol{\lambda}\mathbf{C}_2^{\mathrm{T}} + (\mathbf{C}_2{}^{\mathrm{T}}\mathbf{G}^{\mathrm{T}}\mathbf{D}^{\mathrm{T}}\mathbf{D})^{\mathrm{T}}\mathbf{G}\mathbf{C}_2\boldsymbol{\lambda}\mathbf{C}_2^{\mathrm{T}} = 0 \tag{13c}$$

The gain can be obtained by solving equations.(13a)-(13c) for the direct output feedback.

3. Identification theory for subsystem and primary structure of AMD-controlled systems

3.1. AMD-controlled system matrix

For an n-story shear building with a AMD attached on the lth floor, the equation of the combined system in state-space form can be written as equation (3). Substituting equation (8) into equation (3) gives

$$\dot{\mathbf{X}}(t) = (\mathbf{A} + \mathbf{B}\mathbf{G}\mathbf{C}_2)\mathbf{X}(t) + \mathbf{E}\ddot{x}_g(t) = \bar{\mathbf{A}}\mathbf{X}(t) + \mathbf{E}\ddot{x}_g(t) \tag{14}$$

where $\bar{\mathbf{A}}$ represent the AMD-controlled system matrix, and $\bar{\mathbf{A}} = \mathbf{A} + \mathbf{B}\mathbf{G}\mathbf{C}_2$.

In the situation that the velocity measured on the lth floor in which AMD is located related to the ground, $\dot{x}_{pl}$, is used as direct output feedback response, the gain matrix $\mathbf{G}$ and $\mathbf{C}_2$ can be expressed as

$$\mathbf{G} = [g_v];\ \mathbf{C}_2 = \{0 \quad \dots \quad 0 \quad \dots \quad 0 \mid 0 \quad \dots \quad 1 \quad \dots \quad 0\}_{1\times 2N} \tag{15}$$

where g_v is velocity gain of the lth floor in which AMD is located. From equation (8), the control force is calculated by

$$u(t) = g_v\dot{x}_{pl} \tag{16}$$

And AMD-controlled system matrix can be expressed in detail as

$$\bar{\mathbf{A}} = \mathbf{A} + \mathbf{B}\mathbf{G}\mathbf{C}_2 = \begin{bmatrix} \mathbf{0} & \mathbf{I} \\ -\mathbf{M}^{-1}\mathbf{K} & -\mathbf{M}^{-1}(\mathbf{C} + \mathbf{B}_1\mathbf{G}_v) \end{bmatrix} = \begin{bmatrix} \mathbf{0} & \mathbf{I} \\ -\mathbf{M}^{-1}\mathbf{K} & -\mathbf{M}^{-1}\bar{\mathbf{C}} \end{bmatrix} \tag{17}$$

where

$$\mathbf{G}\mathbf{C}_2 = \{0 \quad \dots \quad 0 \quad \dots \quad 0 \mid 0 \quad \dots \quad g_v \quad \dots \quad 0\}_{1\times 2N} = \{\mathbf{0} \quad \mathbf{G}_v\} \tag{18}$$

3.2. Identification theory

The terms λ_j and $\boldsymbol{\Psi}_j$ denote the jth eigenvalue and its corresponding $2N\times 1$ eigenvector of the system matrix $\bar{\mathbf{A}}$. The physical-domain system matrix is related to the jth eigenparameters by using the state-space characteristic equation

$$(\bar{\mathbf{A}} - \lambda_j\mathbf{I})\boldsymbol{\Psi}_j = \mathbf{0} \tag{19}$$

Substituting equation (17) into equation (19) gives

$$\left\{\begin{bmatrix} \mathbf{0} & \mathbf{I} \\ -\mathbf{M}^{-1}\mathbf{K} & -\mathbf{M}^{-1}\bar{\mathbf{C}} \end{bmatrix} - \lambda_j\begin{bmatrix} \mathbf{I} & \mathbf{0} \\ \mathbf{0} & \mathbf{I} \end{bmatrix}\right\}\boldsymbol{\Psi}_j = 0 \tag{20}$$

Furthermore, the expression of the lower half of equation (20), where contains information regarding the dynamic properties of the system, gives

$$\begin{bmatrix}\mathbf{L} & \mathbf{R}\end{bmatrix}\boldsymbol{\psi}_j = 0 \tag{21}$$

where

$$\mathbf{L}=\begin{bmatrix} -\frac{k_{p_1}+k_{p_2}}{m_{p_1}} & \frac{k_{p_2}}{m_{p_1}} & 0 & \cdots & \cdots & \cdots & 0 \\ \frac{k_{p_2}}{m_{p_2}} & -\frac{k_{p_2}+k_{p_3}}{m_{p_2}} & \frac{k_{p_3}}{m_{p_2}} & 0 & & & \vdots \\ 0 & \ddots & \ddots & \ddots & & & \vdots \\ \vdots & 0 & \frac{k_{p_l}}{m_{p_l}} & -\frac{k_{p_l}+k_{p_{l+1}}+k_s}{m_{p_l}} & \frac{k_{p_{l+1}}}{m_{p_l}} & 0 & \frac{k_s}{m_{p_l}} \\ \vdots & & \ddots & \ddots & \ddots & \vdots & \vdots \\ \vdots & & & 0 & \frac{k_{p_n}}{m_{p_n}} & -\frac{k_{p_n}}{m_{p_n}} & 0 \\ 0 & \cdots & \cdots & \frac{k_s}{m_s} & \cdots & 0 & -\frac{k_s}{m_s} \end{bmatrix} \tag{22a}$$

$$\mathbf{R}=\begin{bmatrix} -\frac{c_{p_1}+c_{p_2}}{m_{p_1}}-\lambda_j & \frac{c_{p_2}}{m_{p_1}} & 0 & \cdots & \cdots & \cdots & 0 \\ \frac{c_{p_2}}{m_{p_2}} & -\frac{c_{p_2}+c_{p_3}}{m_{p_2}}-\lambda_j & \frac{c_{p_3}}{m_{p_2}} & 0 & & & \vdots \\ 0 & \ddots & \ddots & \ddots & & & \vdots \\ \vdots & 0 & \frac{c_{p_l}}{m_{p_l}} & -\frac{c_{p_l}+c_{p_{l+1}}+c_s-g_v}{m_{p_l}}-\lambda_j & \frac{c_{p_{l+1}}}{m_{p_l}} & 0 & \frac{c_s}{m_{p_l}} \\ \vdots & & \ddots & \ddots & \ddots & \vdots & \vdots \\ \vdots & & & 0 & \frac{c_{p_n}}{m_{p_n}} & -\frac{c_{p_n}}{m_{p_n}}-\lambda_j & 0 \\ 0 & \cdots & \cdots & \frac{c_s-g_v}{m_s} & \cdots & 0 & -\frac{c_s}{m_s}-\lambda_j \end{bmatrix} \tag{22b}$$

$$\mathbf{\Psi}_j=\begin{Bmatrix}\psi_{1,j} & \psi_{2,j} & \cdots & \psi_{n,j} & \psi_{N,j} & \cdots & \psi_{2N-1,j} & \psi_{2N,j}\end{Bmatrix}^T \tag{22c}$$

3.2.1. Identification of velocity gain matrix g_v of AMD

From the last row of equation (21),

$$k_s(\psi_{l,j}-\psi_{N,j})+c_s(\psi_{N+l,j}-\psi_{2N,j})-g_v\psi_{N+l,j}=m_s\lambda_j\psi_{2N,j} \tag{23}$$

As $c_s=k_s=0$, the velocity gain matrix g_v of AMD can be obtained and expressed as

$$g_v=\frac{-m_s\lambda_j\psi_{2N,j}}{\psi_{N+l,j}}\ (j=1,2,\ldots,\text{or } 2N) \tag{24}$$

As some components with stiffness and damping are installed in the AMD ($c_s\neq 0$ and $k_s\neq 0$), k_s, c_s and g_v can be derived on the basis of three different complex mode shape and then obtained by

$$\begin{Bmatrix} k_s \\ c_s \\ g_v \end{Bmatrix} = \begin{bmatrix} \psi_{l,j_1} - \psi_{N,j_1} & \psi_{N+l,j_1} - \psi_{2N,j_1} & -\psi_{N+l,j_1} \\ \psi_{l,j_2} - \psi_{N,j_2} & \psi_{N+l,j_2} - \psi_{2N,j_2} & -\psi_{N+l,j_2} \\ \psi_{l,j_3} - \psi_{N,j_3} & \psi_{N+l,j_3} - \psi_{2N,j_3} & -\psi_{N+l,j_3} \end{bmatrix} \begin{Bmatrix} m_s \lambda_{j_1} \psi_{2N,j_1} \\ m_s \lambda_{j_2} \psi_{2N,j_2} \\ m_s \lambda_{j_3} \psi_{2N,j_3} \end{Bmatrix} \tag{25}$$

3.2.2. Identification of the primary building

(1) Damping and stiffness coefficients of the *l*th story in which the AMD is located

To obtain the dynamic parameters of primary building, the derivation begins at the *l*th row of equation (20), and then the damping coefficient of the *l*th story of the primary building can be derived and expressed as

$$\begin{aligned} c_{p_l} = {} & c_{p_{l+1}} \frac{(\psi_{N+l,j} - \psi_{N+l+1,j})}{(\psi_{n+l,j} - \psi_{N+l,j})} + k_{p_{l+1}} \frac{(\psi_{l,j} - \psi_{l+1,j})}{(\psi_{n+l,j} - \psi_{N+l,j})} - k_{p_l} \frac{(\psi_{l-1,j} - \psi_{l,j})}{(\psi_{n+l,j} - \psi_{N+l,j})} \\ & + c_s \frac{(\psi_{N+l,j} - \psi_{2N,j})}{(\psi_{n+l,j} - \psi_{N+l,j})} - g_v \frac{\psi_{N+l,j}}{(\psi_{n+l,j} - \psi_{N+l,j})} + k_s \frac{(\psi_{l,j} - \psi_{N,j})}{(\psi_{n+l,j} - \psi_{N+l,j})} + \frac{\lambda_j \psi_{N+l,j} m_{p_l}}{(\psi_{n+l,j} - \psi_{N+l,j})} \end{aligned} \tag{26}$$

Next, any complex modes can be selected (e.g. *j*th and *k*th modes), and the stiffness coefficient of the *l*th story of the primary structure can be derived on the basis of equation (26) as

$$\begin{aligned} k_{p_l} = {} & \left[\frac{\psi_{l-1,k} - \psi_{l,k}}{\psi_{n+l,k} - \psi_{N+l,k}} - \frac{\psi_{l-1,j} - \psi_{l,j}}{\psi_{n+l,j} - \psi_{N+l,j}} \right]^{-1} \\ & \cdot \left[\frac{\hat{C}_{l+1,k}}{\psi_{n+l,k} - \psi_{N+l,k}} - \frac{\hat{C}_{l+1,j}}{\psi_{n+l,j} - \psi_{N+l,j}} + \frac{\hat{K}_{l+1,k}}{\psi_{n+l,k} - \psi_{N+l,k}} - \frac{\hat{K}_{l+1,j}}{\psi_{n+l,j} - \psi_{N+l,j}} \right. \\ & + \frac{\hat{C}_{s_{l,k}}}{\psi_{n+l,k} - \psi_{N+l,k}} - \frac{\hat{C}_{s_{l,j}}}{\psi_{n+l,j} - \psi_{N+l,j}} + \frac{\hat{K}_{s_{l,k}}}{\psi_{n+l,k} - \psi_{N+l,k}} - \frac{\hat{K}_{s_{l,j}}}{\psi_{n+l,j} - \psi_{N+l,j}} \\ & \left. + \frac{\lambda_k \psi_{N+l,k} m_{p_l}}{\psi_{n+l,k} - \psi_{N+l,k}} - \frac{\lambda_i \psi_{N+l,j} m_{p_l}}{\psi_{n+l,j} - \psi_{N+l,j}} \right] \end{aligned} \tag{27}$$

where $\hat{K}_{l+1,j} = k_{p_{l+1}}(\psi_{l,j} - \psi_{l+1,j})$, $\hat{C}_{l+1,j} = c_{p_{l+1}}(\psi_{N+l,j} - \psi_{N+l+1,j})$, $\hat{K}_{s_{l,j}} = k_s(\psi_{l,j} - \psi_{N,j})$, and $\hat{C}_{s_{l,j}} = c_s(\psi_{N+l,j} - \psi_{2N,j}) - g_v\psi_{N+L,j}$. In equation (27), parameters k_s , c_s and g_v can be solved from equation (24) or equation (25) which determine $\hat{K}_{s_{l,j}}$, $\hat{C}_{s_{l,j}}$, $\hat{K}_{s_{l,k}}$, and $\hat{C}_{s_{l,k}}$. In addition, the information related to the (*l*+1) story (i.e., $\hat{K}_{l+1,j}$, $\hat{C}_{l+1,j}$, $\hat{K}_{l+1,k}$, and $\hat{C}_{l+1,k}$) can be solved in advance (as shown in the next section). The floor masses of the primary building and AMD are assumed to be known, and equations (26) and (27) are then solved sequentially.

(2) Damping and stiffness coefficient of the top story (at which the AMD is not installed)

For the top story, equation (27) can be applied by setting $\hat{K}_{l+1,i} = \hat{K}_{l+1,k} = \hat{C}_{l+1,i} = \hat{C}_{l+1,k} = 0$. In addition, assigning $l = n$ in equation (27) lead to

$$k_{p_n}=\left[\frac{\psi_{n-1,k}-\psi_{n,k}}{\psi_{2n,k}-\psi_{2N-1,k}}-\frac{\psi_{n-1,j}-\psi_{n,j}}{\psi_{2n,j}-\psi_{2N-1,j}}\right]^{-1}\cdot\left[\frac{\lambda_k\psi_{2N-1,k}m_{p_n}}{\psi_{2n,k}-\psi_{2N-1,k}}-\frac{\lambda_i\psi_{2N-1,j}m_{p_n}}{\psi_{2n,j}-\psi_{2N-1,j}}+\frac{\hat{C}_{s_{n,k}}}{\psi_{2n,k}-\psi_{2N-1,k}}-\frac{\hat{C}_{s_{n,j}}}{\psi_{2n,j}-\psi_{2N-1,j}}+\frac{\hat{K}_{s_{n,k}}}{\psi_{2n,k}-\psi_{2N,k}}-\frac{\hat{K}_{s_{n,j}}}{\psi_{2n,j}-\psi_{2N-1,j}}\right] \tag{28}$$

Furthermore, setting $c_{p_{l+1}}=k_{p_{l+1}}=0$ and $l=n$ in equation (26) gives

$$c_{p_n}=-k_{p_n}\frac{(\psi_{n-1,j}-\psi_{n,j})}{(\psi_{2n,j}-\psi_{N+n,j})}+\frac{\lambda_j\psi_{N+n,j}m_{p_n}}{(\psi_{2n,j}-\psi_{N+n,j})}+c_s\frac{(\psi_{N+n,j}-\psi_{2N,j})}{(\psi_{2n,j}-\psi_{N+n,j})}+k_s\frac{(\psi_{n,j}-\psi_{N,j})}{(\psi_{2n,j}-\psi_{N+n,j})} \tag{29}$$

In a situation in which the AMD is not installed at the *n*th story, then k_s, c_s, $\hat{K}_{s_{n,j}}$ $\hat{C}_{s_{n,j}}$ $\hat{K}_{s_{n,k}}$ $\hat{C}_{s_{n,k}}$ are all equal to zero. The Damping and stiffness coefficient of the top story can be calculated by

$$k_{p_n}=\left[\frac{\psi_{n-1,k}-\psi_{n,k}}{\psi_{2n,k}-\psi_{2N-1,k}}-\frac{\psi_{n-1,j}-\psi_{n,j}}{\psi_{2n,j}-\psi_{2N-1,j}}\right]^{-1}\left[\frac{\lambda_k\psi_{2N-1,k}m_{p_n}}{\psi_{2n,k}-\psi_{2N-1,k}}-\frac{\lambda_i\psi_{2N-1,j}m_{p_n}}{\psi_{2n,j}-\psi_{2N-1,j}}\right] \tag{30}$$

$$c_{p_n}=-k_{p_n}\frac{(\psi_{n-1,i}-\psi_{n,i})}{(\psi_{2n,i}-\psi_{N+n,i})}+\frac{\lambda_i\psi_{N+n,i}m_{p_n}}{(\psi_{2n,i}-\psi_{N+n,i})} \tag{31}$$

(3) Damping and stiffness coefficient of the other inner story (at which the AMD is not installed)

Equations (26) and (27) can be applied to calculate the stiffness and damping coefficient of the other inner story (the *i*th story), at which the AMD is not installed, by setting $k_s=c_s=g_v=0$. The following equation can be derived

$$k_{p_i}=\left[\frac{\psi_{i-1,k}-\psi_{i,k}}{\psi_{n+i,k}-\psi_{N+i,k}}-\frac{\psi_{i-1,j}-\psi_{i,j}}{\psi_{n+i,j}-\psi_{N+i,j}}\right]^{-1}\cdot\left[\frac{\hat{C}_{i+1,k}}{\psi_{n+i,k}-\psi_{N+i,k}}-\frac{\hat{C}_{i+1,j}}{\psi_{n+i,j}-\psi_{N+i,j}}+\frac{\hat{K}_{i+1,k}}{\psi_{n+i,k}-\psi_{N+i,k}}-\frac{\hat{K}_{i+1,j}}{\psi_{n+i,j}-\psi_{N+i,j}}+\frac{\lambda_k\psi_{N+i,k}m_{p_i}}{\psi_{n+i,k}-\psi_{N+i,k}}-\frac{\lambda_i\psi_{N+i,j}m_{p_i}}{\psi_{n+i,j}-\psi_{N+i,j}}\right] \tag{30}$$

$$c_{p_i}=c_{p_{i+1}}\frac{(\psi_{N+i,j}-\psi_{N+i+1,j})}{(\psi_{n+i,j}-\psi_{N+i,j})}+k_{p_{i+1}}\frac{(\psi_{i,i}-\psi_{i+1,j})}{(\psi_{n+i,j}-\psi_{N+i,j})}-k_{p_i}\frac{(\psi_{i-1,j}-\psi_{i,j})}{(\psi_{n+i,j}-\psi_{N+i,j})}+\frac{\lambda_j\psi_{N+i,j}m_{pi}}{(\psi_{n+i,j}-\psi_{N+i,j})} \tag{31}$$

(4) Damping and stiffness coefficient of the first story (at which the AMD is not installed)

For the first story (i.e., when $l=1$), $\psi_{l-1,i}$, $\psi_{l-1,k}$, $\psi_{n+l,i}$, and $\psi_{n+l,k}$ are eliminated and are all equal to zero in equations (26) and (27). The following equation can be derived

$$k_{p_1}=\left[\frac{\psi_{1,k}}{\psi_{N+1,k}}-\frac{\psi_{1,j}}{\psi_{N+1,j}}\right]^{-1}\cdot\left[-\frac{\hat{C}_{1+1,k}}{\psi_{N+1,k}}+\frac{\hat{C}_{1+1,j}}{\psi_{N+1,j}}-\frac{\hat{K}_{1+1,k}}{\psi_{N+1,k}}+\frac{\hat{K}_{1+1,j}}{\psi_{N+1,j}}-\lambda_k m_{p_1}+\lambda_j m_{p_1}\right] \tag{32}$$

$$c_{p_1} = c_{p_2}\frac{\psi_{N+2,j}-\psi_{N+1,j}}{\psi_{N+1,j}} + k_{p_2}\frac{\psi_{2j}-\psi_{1,j}}{\psi_{N+l,j}} - k_{p_1}\frac{\psi_{1,j}}{\psi_{N+1,j}} - \frac{\lambda_j\psi_{N+1,j}m_{p_1}}{\psi_{N+1,j}} \tag{33}$$

3.3. Identification Procedure

The following analysis procedure is used for extracting the feedback gain of the AMD controller and the dynamic properties of the primary building for displacement and velocity feedback: 1) The masses of each floor and AMD are known. ; 2) The acceleration response of each floor and AMD are needed to be measured for AMD-controlled system. ; 3) To identify the eigenvalues and eigenvectors from the acceleration measurements of the building-AMD system, the System Realization Using Information Matrix (SRIM) identification technique [14-17] is employed based on the selected system input and output measurements for the input–output situation. Regarding the output-only situation, the stochastic subspace identification (SSI)[17, 18] method is employed on the basis of the output response of the building–AMD system. Transforming discrete time into continuous time may obtain the optimal realization of the state–space system matrix $\overline{\mathbf{A}}$. The continuous-time eigenvalue λ_j and eigenvector $\mathbf{\Psi}_j$ of system matrix $\overline{\mathbf{A}}$ are computed. ; 4) In the situation of $c_s = k_s = 0$, the velocity feedback gain of AMD can be obtained from equation (24) based on selecting one set of eigenparameters within the second mode or the higher-mode. Whereas some components with stiffness and damping are installed in the AMD ($c_s \neq 0$ and $k_s \neq 0$), k_s, c_s and g_v can be obtained from equation (25) by selecting three sets of eigenparameters. ; 5) According to the equations in Section 3.2.2, the stiffness and damping coefficient of each floor can be obtained by selecting any two sets of eigenparameters complex modes

4. Numerical verifications

To verify the accuracy of the aforementioned methodology, numerical studies for two three-story building were conducted. The primary structure of the first case (CASE-1) is a shear-type building, whereas the structure of the second case (CASE-2) is a real benchmark building, for which the damping and stiffness matrices are full matrices, The structural parameters of CASE-2 were synthesized from a modal testing performed on an actual 3-story steel frame erected in the earthquake simulation laboratory of the National Center for Research on Earthquake Engineering (NCREE) in Taipei, Taiwan. The physical and normal-modal parameters of these two buildings are presented in Tables 1 and 2. The accuracy of the proposed parameter-extraction procedure was investigated using different building types to examine its applicability to evaluating AMD performance in real building-AMD structures.

An AMD with a mass of 360 kg was assumed. The AMD was assumed to be installed on the roof (third floor) of the building. The stiffness and damping coefficient of AMD are 1 kN/m and 0.1 kN-sec/m, respectively. According to optimal H_∞ control algorithm in Section 2, the velocity gains of the AMD on the roof floor were designed as $g_v = -4389$ for CASE-1 and $g_v = -4756$ for CASE-2, respectively. For input-output situation, the ground acceleration recorded at National Chung Hsing University (NCHU) in the east-west direction during the 1999 Taiwan Chi-Chi earthquake was used as the base excitation. Figures 2 and 3 show the acceleration responses of the roof floor under the ground motion of the 1999 Taiwan Chi-Chi earthquake with and without AMD.

Table 3 presents the obtained parameters of the AMD and primary building by using the proposed method. As shown in Table 3, $\{\hat{\omega}_{0_1}, \hat{\omega}_{0_2}, \hat{\omega}_{0_3}\}$ and $\{\hat{\xi}_{0_1}, \hat{\xi}_{0_2}, \hat{\xi}_{0_3}\}$ were the identified real modal frequencies and damping ratios of the reconstructed shear building based on $\{\hat{c}_{p_1}, \hat{c}_{p_2}, \hat{c}_{p_3}\}$ and $\{\hat{k}_{p_1}, \hat{k}_{p_2}, \hat{k}_{p_3}\}$. In theory, the proposed method can be implemented by selecting any two sets of eigenvalues and eigenvectors, namely (λ_j, $\mathbf{\Psi}_j$) and (λ_k, $\mathbf{\Psi}_k$). The results of CASE-1 showed that the

identified parameters of the AMD and primary building were the same as the original parameters (Table 2), regardless of the selection of (*j*, *k*) set. For CASE-2, the parameters of the AMD and primary building were also accurately identified regardless of the selection of (*j*, *k*) set. The results showed that the identified "pseudoshear" building was related to the selection of (*j*, *k*); it was difficult to assess which set of the identified physical parameters could optimally represent the CASE-2 building. However, although the modal parameters of the reconstructed shear building could not fully represent the original building, selecting the (j, k) pairs resulted in the optimal estimation of the corresponding building mode. Specifically, selecting (*j*, *k*) = (1, 2) or (3, 4) resulted in the optimal $\hat{\omega}_{0_1}$ and $\hat{\xi}_{0_1}$, selecting (*j*, *k*) = (5, 6) resulted in the optimal $\hat{\omega}_{0_2}$ and $\hat{\xi}_{0_2}$, and continued in a trend of optimally selected pairs and resulting estimations. These results indicate that it is always possible to obtain modal parameters of a building that are more accurate by selecting various (*j*, *k*) pairs.

Table 1. Physical parameters of two 3-story buildings in the numerical study.

Physical parameters	CASE-1：Ideal shear building	CASE-2: NCREE benchmark building
Mass matrix (kg)	$\begin{bmatrix} 6000 & 0 & 0 \\ 0 & 6000 & 0 \\ 0 & 0 & 6000 \end{bmatrix}$	$\begin{bmatrix} 6000 & 0 & 0 \\ 0 & 6000 & 0 \\ 0 & 0 & 6000 \end{bmatrix}$ 1F 2F 3F
Damping matrix (*kN*-sec/m)	$\begin{bmatrix} 13.6 & -7.90 & 0 \\ -7.90 & 13.3 & -5.40 \\ 0 & -5.40 & 5.40 \end{bmatrix}$	$\begin{bmatrix} 13.28 & -8.701 & 1.463 \\ -8.701 & 13.557 & -5.774 \\ 1.463 & -5.774 & 5.657 \end{bmatrix}$ 1F 2F 3F
Stiffness matrix (kN/m)	$\begin{bmatrix} 3300 & -1600 & 0 \\ -1600 & 3100 & -1500 \\ 0 & -1500 & 1500 \end{bmatrix}$	$\begin{bmatrix} 3406 & -1814 & 138.2 \\ -1814 & 3329 & -1672 \\ 138.2 & -1672 & 1509 \end{bmatrix}$ 1F 2F 3F

Table 2. Real modal parameters of two 3-story buildings in the numerical study.

Modal parameters	CASE-1：Ideal shear building	CASE-2: NCREE benchmark building
Frequency, (Hz) $\{\omega_{0_1} \quad \omega_{0_2} \quad \omega_{0_3}\}$	$\{1.17 \quad 3.22 \quad 4.65\}$	$\{1.04 \quad 3.17 \quad 4.86\}$
Damping ratio, (%) $\{\xi_{0_1} \quad \xi_{0_2} \quad \xi_{0_3}\}$	$\{1.45 \quad 3.65 \quad 6.32\}$	$\{1.99 \quad 3.07 \quad 6.43\}$
Mode shape, $\{\boldsymbol{\varphi}_{0_1} \quad \boldsymbol{\varphi}_{0_2} \quad \boldsymbol{\varphi}_{0_3}\}$	$\begin{bmatrix} 0.421 & -1.194 & 2.124 \\ 0.783 & -0.634 & -2.420 \\ 1.000 & 1.000 & 1.000 \end{bmatrix}$	$\begin{bmatrix} 0.408 & -1.247 & 1.954 \\ 0.784 & -0.627 & -2.291 \\ 1.000 & 1.000 & 1.000 \end{bmatrix}$ 1F 2F 3F

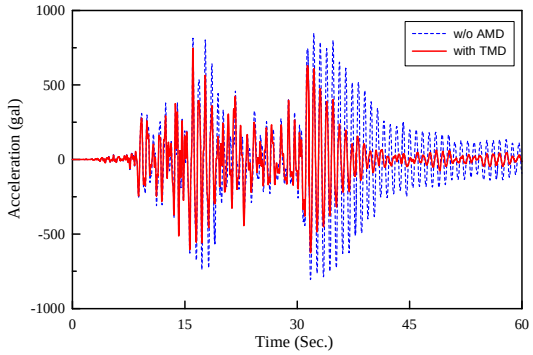

Figure 2. Roof acceleration response with and without AMD for CASE-1.

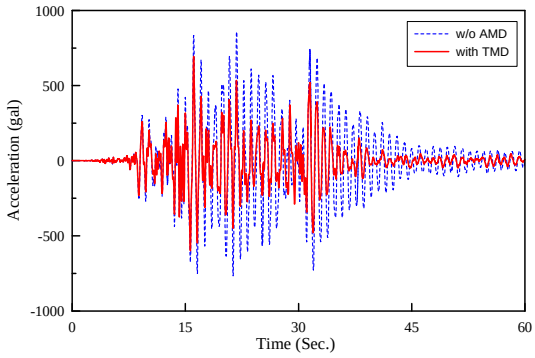

Figure 3. Roof acceleration response with and without AMD for CASE-2.

Table 3. Identified parameters of the AMD and primary buildings in the numerical study

Identified Parameters		(j_1, j_2, j_3) or (j, k)	CASE-1	CASE-2
AMD	$\hat{g}_v$	(1,2,3)、(4,5,6)	-4387	-4756
	$\hat{k}_s\,(kN/m)$	(1, 2)、(3, 4)	1	1
	$\hat{c}_s\,(k\text{N-sec/m})$	(5, 6)、(7, 8)	0.1	0.1
Primary building (physical)	$\{\hat{c}_{p_1}, \hat{c}_{p_2}, \hat{c}_{p_3}\}$ (kN-sec/m)	(1, 2)	{5.7, 7.9, 5.4}	{8.55, 7.86, 6.71}
		(3, 4)		{8.28, 8.12, 5.31}
		(5, 6)		{4.67, 6.37, 4.50}
		(7, 8)		{7.79, 7.58, 6.58}
	$\{\hat{k}_{p_1}, \hat{k}_{p_2}, \hat{k}_{p_3}\}$ (kN/m)	(1, 2)	{1700, 1600, 1500}	{1326, 1187, 1301}
		(3, 4)		{1367, 1206, 1179}
		(5, 6)		{1672, 1431, 1465}
		(7, 8)		{1901, 1704, 1704}
Primary building (modal)	$\{\hat{\omega}_{0_1}, \hat{\omega}_{0_2}, \hat{\omega}_{0_3}\}$ (Hz)	(1, 2)	{1.17, 3.22, 4.65}	{**1.03**, 2.92, 4.13}
		(3, 4)		{**1.04**, 2.86, 4.08}
		(5, 6)		{1.14, **3.17**, 4.49}
		(7, 8)		{1.23, 3.41, **4.86**}
	$\{\hat{\xi}_{0_1}, \hat{\xi}_{0_2}, \hat{\xi}_{0_3}\}$ (%)	(1, 2)	{1.45, 3.65, 6.32}	{**2.07**, 5.32, 7.84}
		(3, 4)		{**1.99**, 4.69, 7.63}
		(5, 6)		{1.24, **3.07**, 5.32}
		(7, 8)		{1.62, 4.28, **6.43**}

5. Conclusions

In this paper, an analysis procedure was developed for extracting the dynamic parameters of an AMD and primary building based on acceleration measurements of a combined building-AMD system. This procedure was first performed by identifying the eigenvalues and eigenvectors from the acceleration measurements of the building-AMD system. These complex eigenparameters were then used to calculate the respective parameters of the AMD and primary building by using the derived analytical formulas. Although the developed theory is based on the shear building assumption, the numerical-simulation results show that the extracted AMD parameters are influenced little by the building model, whereas the building parameters of different modes can be accurately extracted by selecting appropriately complex modes. It is concluded that the proposed analysis procedure can be appropriately

applied to the health monitoring of a combined building-AMD system and used for ensuring the performance of the AMD control system.

Acknowledgements
This work is supported by the Ministry of Science and Technology of the Republic of China (Taiwan) under grants No. 104-2625-M-492 -013. This supports is greatly appreciated.

References

[1] Soong T T and Cimellaro G P 2009 Future directions in structural control *Structural Control and Health Monitoring* vol 16 pp 7-16
[2] Korkmaz S 2011 A review of active structural control: challenges for engineering informatics *Journal Computers and Structures archive* Vol 89 pp 2113-2132
[3] Chung L L, Reinhorn A M and Soong T T 1988 Experiment on active control of seismic structures *Journal of Engineering Mechanics* (ASCE) vol 114 pp 241-256
[4] Indrawan B, Kobori T, Sakamoto M, Koshika N, and Ohrui S 1996 Experimental verification of bound-force control method *Earthquake Engineering and Structural Dynamics* vol 25 pp 179-193
[5] Chung L L, Lin C C and Chu S Y 1993 Optimal Direct Output Feedback of Structural Control *Journal of Engineering Mechanics* (ASCE) vol 119 pp 2157-2173
[6] Lin C C, Chung L L, and Lu K H 1996 Optimal Discrete-time Structural Control Using Direct Output Feedback *Engineering Structures* vol 18 pp 472-482.
[7] Kobori T, Koshika N, Yamada K, Ikeda Y 1991 Seismic-response-controlled structure with active mass driver system. part 1: design *Earthquake Engineering and Structural Dynamic* vol 20 pp 133-149
[8] Yao J T P 1972 Concept of structure control *Journal of Structural Engineering* (ASCE) vol 98 pp 1567-1574
[9] Ikeda Y, Sasaki K, Sakamoto M and Kobori T 2001 Active mass driver system as the first application of active structural control *Earthquake Engineering and Structural Dynamic* vol 30 pp 1575-1595
[10] Wu J C, Yang J N, and Schmitendorf W E 1998 Reduced-order and LQR Control for Wind-excited Tall Buildings *Engineering Structures* vol 20 pp 222-236
[11] Lin C C, Chang C C, Chen H L 2006 Optimal Output Feedback Control System with Time Delay *Journal of Engineering Mechanics* (ASCE) vol 132 pp1096-1105
[12] Lin C C and Chang C C 2013 Optimum Design Strategy of Time-Delayed Velocity Feedback Control *Journal of Engineering Mechanics* (ASCE) vol 139 pp 1460-1469.
[13] Chu S Y, Lin C C, Chung L L, Chang C C, and Lu K H 2008 Optimal Performance of Discrete-time Direct Output Feedback Structural Control with Delayed Control Forces *Structural Control and Health Monitoring* vol 5 pp 20-42
[14] Juang J N 1997 System realization using information matrix *Journal of Guidance, Control, and Dynamics* vol 21 pp 492-500
[15] Lin C C, Wang C E, Wu H W and Wang J F 2005 On-line building damage assessment based on earthquake records *Smart Materials and Structures* vol 14 S137-S153
[16] Lin C C, Wang J F and Tsai C H 2008 Dynamic parameter identifications for irregular buildings considering soil-structure interaction effects *Earthquake Spectra* vol 24 pp 641-666.
[17] Wang J F and Lin C C 2015 Extracting parameters of TMD and primary structure from the combined system responses *Smart Structures and Systems* vol 16 pp 937-960
[18] Van Overschee P and De Moor B 2011 *Subspace Identification for Linear Systems: Theory Implementation-Applications* (New York: Springer)